Studies on the Preparation of Immersion-Type Polypropylene Fragrant Fiber. II. The Supermolecular Structure of the Matrix Fiber and Its Sorption Properties for Fragrant Molecules

Wang Bing, Zhao Jiasen

School of Material Science and Chemical Engineering, Tianjin Polytechnic University, Tianjin 300160, People's Republic of China

Received 23 August 2002; accepted 22 November 2002

ABSTRACT: The supermolecular structure and mechanical properties of a matrix fiber were investigated with differential scanning calorimetry, wide-angle X-ray diffraction, sonic velocity instrumentation, and fiber electronic serimetry. The results indicated that the apparent crystallinity of the matrix fiber, the crystallinity of the polypropylene (PP) component, and the mechanical properties of the matrix fiber were all affected by ethylene vinyl acetate (EVA). Drawing increased the orientation and tensile strength of the matrix fiber at the proper temperature and ratio of PP to EVA. The matrix fiber, having good mechanical properties, was placed in a fragrance–alcohol solution or an essential oil for the preparation of a fragrant fiber. The fragrance property of the fiber was determined with generally a method using slow release time as a certain standard, and the results showed that the fragrance property of the fiber was good. © 2003 Wiley Periodicals, Inc. J Appl Polym Sci 90: 973–981, 2003

Key words: poly(propylene) (PP); mechanical properties; adsorption; fibers

INTRODUCTION

Property modification has been the main trend in synthetic fiber science and technology in recent years. The blending of two or more polymers to produce new material systems with a combination of properties for specific uses has extensively been developed in several industries as a way of meeting new market applications with minimum cost.[1–4] At present, the preparation of polypropylene (PP) fragrant fibers is performed with a blend-spinning method involving PP and aromatics or fragrant microcapsules. Many fragrant textile products have been produced with fragrant fibers, such as fragrant bat wool, fragrant handkerchiefs, fragrant curtains, and fragrant neckties.[5–10] The spicery is slowly released from the fragrant textile products and may dispel a person's weariness, optimize the environment, disinfect, and diminish inflammation. Ethylene vinyl acetate (EVA) is a very interesting material with excellent ozone and weather resistance, good toughness at low temperatures, and oil-absorbent properties.[11–15] In a previous article, we reported that the PP/EVA matrix fiber could be prepared by a combination of a thermoplastic, spin-fiber-forming polymer and an oil-absorbent resin. We now report studies on the supermolecular structure, mechanical properties, and adsorption properties of the matrix fiber.

Correspondence to: W. Bing (hxl_009@sina.com).

Journal of Applied Polymer Science, Vol. 90, 973–981 (2003)

EXPERIMENTAL

Materials

PP (melt index = 17–18 g/min, melting temperature = 171.18°C) was made at the Liaoyang Petroleum and Chemical Fiber Plant (Liaoyang, China). EVA [vinyl acetate content = 30 ± 2% (as determined by saponification), melting temperature = 81°C] was made at the Shanghai Chemical Engineering Institute (Shanghai, China).

Preparation of the matrix blends

Particles of EVA and PP were dried and placed in an SJ-20 Z×25 plastic extruder (Beijing Extruding Plant, Beijing, China), in which a spinning jet was equipped with a static mixer to spin through a cool water bath. The PP/EVA blends were cut into 3-mm-long particles, dried, cooled, and placed in the drier.

Scanning electron microscopy of the PP/EVA matrix blends

The PP/EVA blends (90/10 PP/EVA) were placed in methyl benzene to sculpture the EVA, were broken in

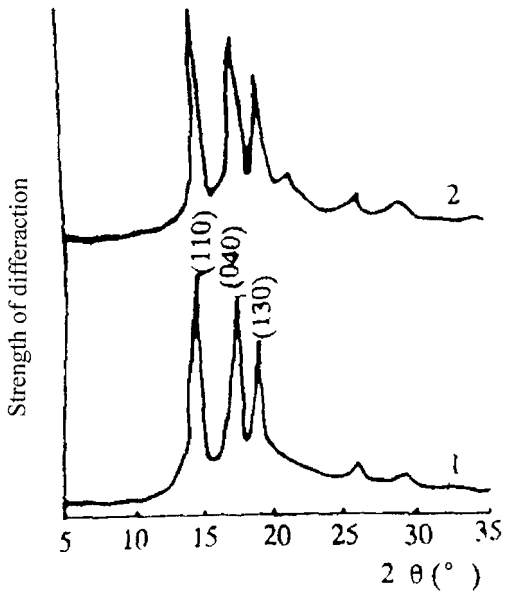

Figure 1 WAXD patterns of as-spun matrix fibers: (1) 10/90 EVA/PP and (2) 20/80 EVA/PP.

liquid nitrogen, and were gilded with sputter-coating film equipment. The microstructures of the surfaces and cross sections of the PP/EVA blends were observed with an S650 scanning electron microscope (Hitachi Co., Japan).

Preparation of the matrix fiber

We spun PP and different compositions of PP/EVA blends in a self-made microplunger frame with melt spinning by an extrusion method. The spinneret plate was homogeneous with six pores, and the diameter of each pore was 0.3 mm. The range of the melt-spinning temperatures of the PP/EVA blends was 220–250°C. The ratio of the pump delivery to the winding speed, which seriously affected the stability of the PP/EVA melt spinning, was from 70/500 to 70/400, according to the different EVA contents.

Drawing of the matrix fiber

The drawing of the as-spun matrix fiber was carried out at 95–100°C on a self-made drawing machine. The drawing range was 1.5–3.5

Heat treatment

The drawn matrix fiber, the drawing range of which was 1.5–3.5, was dried and heat-treated at 120–122°C for 10 min.

Orientation measurements by the sonic velocity method

The orientation factor of the sonic velocity was determined from the transit time of a sound pulse between two transducers coupled to the specimens. The measurements were made with an SSY-I fiber sonic velocity meter (Siping Electronic Instrument Plant, Siping, China). From the measured sonic velocity (C), the orientation factor of the samples (f_s) was calculated as follows:

$$f_s = 1 - (C_u/C)^2 \quad (1)$$

where C_u is the sonic velocity of a fully unoriented sample.

X-ray diffraction measurements

A matrix fiber sample was wound into a bunch. Its wide-angle X-ray diffraction (WAXD) spectrum was recorded with a Rigaku Dmax+A X-ray diffraction instrument (Rigaku Co., Japan) at 35 kV and 20 mA. The X-rays were monochromatized with a nickel filter to obtain Cu Kα radiation.

Thermal behavior measurements

The melting behavior of the matrix blending fiber was investigated with a PerkinElmer DSC-2C differential scanning calorimeter (Perkin Elmer Co., USA) in a nitrogen atmosphere. An empty sample pan was taken as the reference sample. The samples were cut into small pieces, weighed accurately at 8 ± 0.5 mg, and heated to 500 K at a heating rate of 20 K/min.

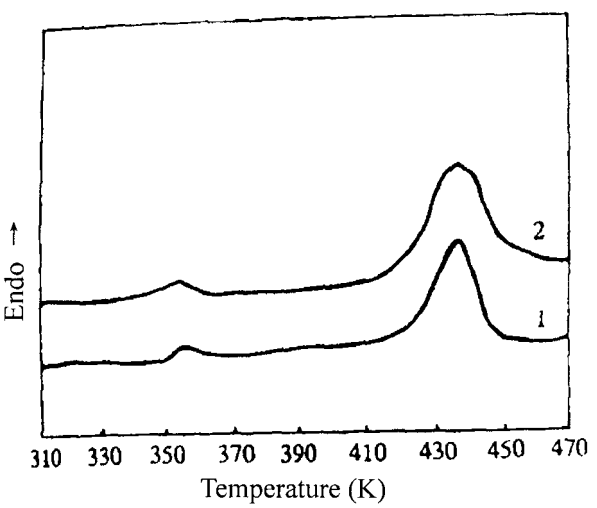

Figure 2 DSC curves of as-spun matrix fibers: (1) 10/90 EVA/PP and (2) 20/80 EVA/PP.

TABLE I
DSC Crystallinity and WAXD Crystallinity of As-Spun Matrix Fibers

PP/EVA	DSC apparent crystallinity	DSC crystallinity of the PP component	WAXD apparent crystallinity	WAXD crystallinity of the PP component
100/0	0.584	0.584	0.699	0.699
95/5	0.552	0.581	0.669	0.704
90/10	0.527	0.586	0.657	0.730
80/20	0.506	0.633	0.627	0.784

DSC crystallinity was determined with the DSC method; WAXD crystallinity was determined with the WAXD method.

Mechanical property test of the matrix fiber

A YG001A fiber electronic serimeter (Nanjing Textile Instrument Plant, Nanjing, China) was used to test the mechanical properties of the single matrix blend fiber. The measurement range was 0–100 CN. The descendant speed range was 10–60 mm/min, the original length of a single fiber was 10 mm, the temperature was 25°C, and the relative humidity was 65%.

Sorption properties of the matrix fiber measurements

The matrix fiber was dipped into perfume molecules in an absolute alcohol solution, and the sorption amount of the perfume molecules into the matrix fiber was determined after a definite time. The amount of sorption (τ) was calculated as follows:

$$\tau = (C_0 - C_t)/W \quad (2)$$

where C_0 is the initial content of perfume molecules in the alcohol solution, C_t is the residual content of perfume molecules when the matrix fiber is dipped into the immersion solution, and W is the weight of the matrix fiber.

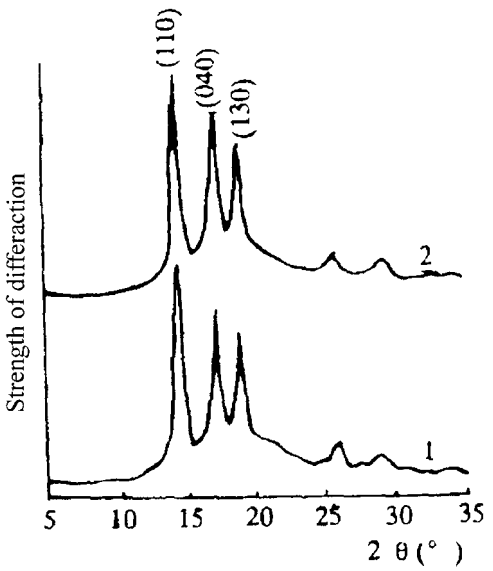

Figure 3 WAXD patterns of posttreatment matrix fibers: (1) 10/90 EVA/PP and (2) 20/80 EVA/PP.

Preparation of the fragrant fiber

The matrix fiber was placed in a perfume absolute alcohol solution or an essential oil to adsorb perfume molecules. After adsorption equilibrium, the fiber was taken out, washed, and dried, and it became a fragrant fiber.

RESULTS AND DISCUSSION

Crystal structure of the matrix fiber

Figure 1 shows the WAXD patterns of the as-spun matrix fiber. The crystallization structure of the matrix fiber was the α-crystal form,[16] and its characteristic 2θ peaks were at 14, 16.8, and 18.4°. The (131) diffraction peak at 21.2° and the (111) diffraction peak at 22.1° mainly appeared at an angle of 45° to the tensile shaft, and there was no diffraction in the direction of the equator because of the high degree of orientation of the matrix fiber. The WAXD spectrogram of an 80/20 PP/EVA matrix fiber could be decomposed into a WAXD atlas of EVA and a WAXD atlas of PP. For EVA(200), 2θ was 23.5°; for EVA(110), 2θ was 21.2°. The difference between the 2θ values of the two diffraction surfaces was only 2.4°. Only a single weak peak appeared at 21° in the WAXD atlas. Because the

TABLE II
Effect of the Drawing Ratio on the Crystallinity of the Matrix Fiber

Drawing ratio	DSC apparent crystallinity	WAXD apparent crystallinity
0	0.528	0.668
1.5	0.527	0.640
2.0	0.538	0.670
2.5	0.552	0.714
3.0	0.581	0.724
3.5	0.578	0.719

The heat-treatment temperature of the drawn matrix fiber (EVA/PP = 90/10) was 120°–122°C: DSC crystallinity was determined with DSC method; WAXD crystallinity was determined with WAXD method.

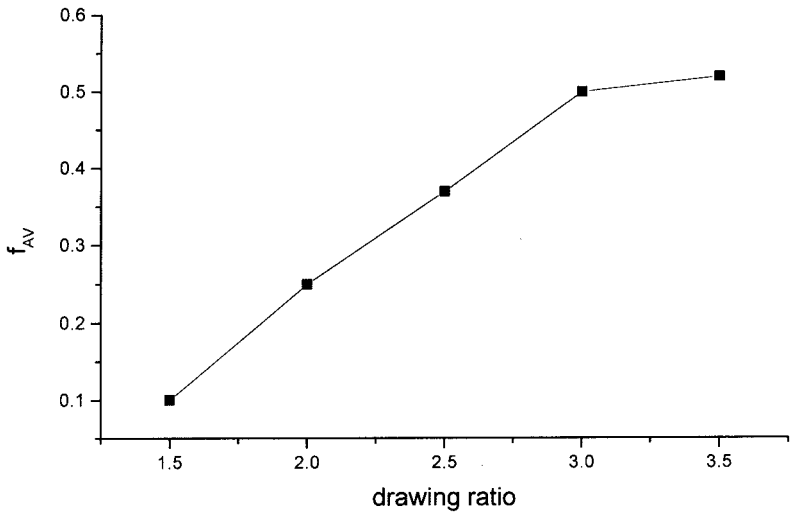

Figure 4 Effects of the drawing ratio on the average orientation degree of the matrix fiber. The measurement sample was the matrix fiber (90/10 EVA/PP).

content of EVA in a 90/10 PP/EVA matrix fiber was much lower, we could not even find its characteristic peak. It could be concluded that EVA and PP crystallized into their crystal structures in the PP/EVA matrix fiber because the characteristic peaks of EVA and PP did not change. Differential scanning calorimetry (DSC) curves of as-spun matrix fibers with different EVA contents are shown in Figure 2. The DSC spectrogram of the EVA/PP matrix fiber was a composition of both the EVA spectrogram and the PP spectrogram, and the melting points of the two components did not change. This conclusion was compatible with the WAXD results. The changes in the crystallinity of the as-spun matrix fibers with different EVA contents are shown in Table I. EVA made the apparent crystallinity of the matrix fiber decrease, but the apparent crystallinity of the PP component increased. The PP component was apt to crystallize in the PP/EVA matrix fiber because of the plasticization of EVA. The WAXD patterns of the posttreatment matrix fibers, which had a drawing ratio of 2.0, a heat-treatment temperature of 120°C, and different EVA contents, are shown in Figure 3. The characteristic 2θ peaks of the posttreatment matrix fiber were still at 14, 16.8, and 18.4°, and the crystal structure was the α-crystal form. The posttreatment did not change the crystal form of the matrix fiber. It was related to the shaping speed of the as-spun fibers. The effects of the drawing ratio on the crystallinity of the matrix fiber are shown in Table II. At the appropriate draw ratio of the matrix fiber, the crystallinity increased with an increase in the extension ratio of the fiber. The crystallinity of the matrix fiber decreased when the extension ratio was too high or too low. During the process of thermal drawing, the partial crystallinity of the PP component, particularly the spherocrystal, was destroyed by the stress and

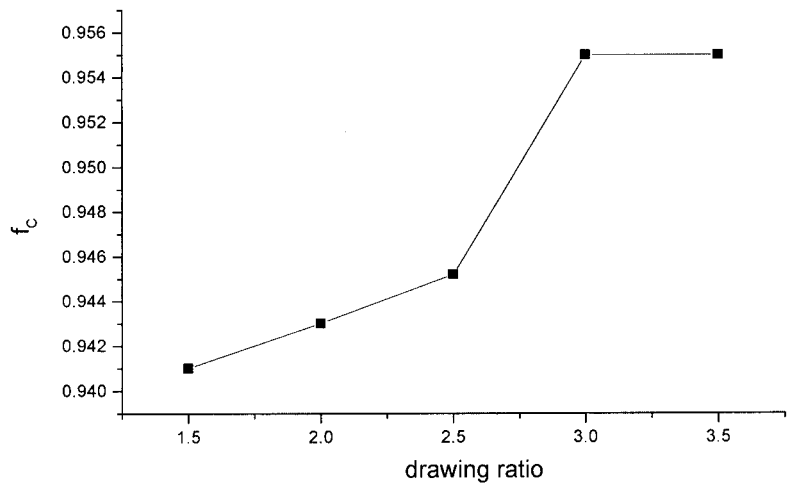

Figure 5 Effects of the drawing ratio on the orientation degree of the crystal area of the matrix fiber. The measurement sample was the matrix fiber (90/10 EVA/PP).

TABLE III
Effects of EVA Content on Mechanical Properties of the Matrix Fiber

PP/EVA	Breaking strength (cN/D)	Extension at break (%)	Initial modulus (cN/D)	Yield strength (cN/D)	Yield strain (%)
100/0	1.81	267	7.26	1.17	25.5
95/5	1.48	264	6.80	1.05	26.38
90/10	1.46	249	6.78	1.02	28.14
80/20	1.07	218	5.36	0.73	30.00

The drawing ratio of the matrix fiber was 0.

temperature, the macromolecular segments oriented along the direction of the axis in the amorphous area, and the partial macromolecular segments built into the crystal lattice to crystallize. In an appropriate range of drawing ratios, both the crystal nucleation ratio and the crystal growth rate were greater than the crystal destruction ratio. When the drawing ratio was too high, the crystal destruction ratio was bigger than the crystal growth ratio, and when the drawing ratio was too low, the crystal growth rate decreased without a crystal inductive effect and led to a crystallinity decrease.

Oriented structure of the matrix fiber

The effects of the drawing ratio on the average orientation degree of the matrix fiber are shown in Figure 4. The effects of the drawing ratio on the orientation degree of the crystal area of the matrix fiber are shown in Figure 5. The relationship curves for the average orientation degree of the matrix fiber, the orientation degree of the crystal area, and the drawing ratio are shown as broken lines, and all transition points appeared at a drawing ratio of 3.0. In addition to the transition points, the degree of orientation increased with an increase in the drawing ratio. The degree of orientation generally did not change with the drawing ratio and reached its maximum after the transition point. In structure, this transition point was compared to the point at which the PP component spherocrystal structure turned into a microfiber structure, the macromolecules were highly oriented, and the degree of orientation reached its maximum.

TABLE IV
Effects of Drawing Ratio on the Mechanical Properties of the Matrix Fiber

Drawing ratio	Breaking strength (cN/D)	Extension at break (%)	Yield strength (cN/D)
0	1.46	249	1.02
1.5	1.89	116	1.74
2.0	2.57	72	2.46
2.5	3.44	42	3.35
3.0	4.26	9	4.26
3.5	6.47	2	6.47

The measurement sample was the matrix fiber (EVA/PP = 90/10).

Mechanical properties of the matrix fiber

The changes in the mechanical properties of the matrix fiber with different EVA contents are shown in Table III. The presence of EVA reduced the breaking strength, extension at break, initial modulus, and yield strength of the matrix fiber and increased the yield strain. Because the interaction force between the EVA phase and PP phase was weaker than the interaction force among PP macromolecules, a stress concentration was produced in the matrix fiber, and the mechanical properties decreased. The changes in the mechanical properties of the matrix fiber (90/10 PP/EVA) with the drawing ratio are shown in Table IV. Drawing increased the breaking strength and yield strength of the matrix fiber and reduced the extension at break. The results may be attributed to the number of molecular segments that could bear the stress in the fiber increasing, and it led to an increase in the break strength. The yield strain was plastic deformation. With an increase in the degree of orientation, the angle between the mean orientation direction of the macromolecular segments

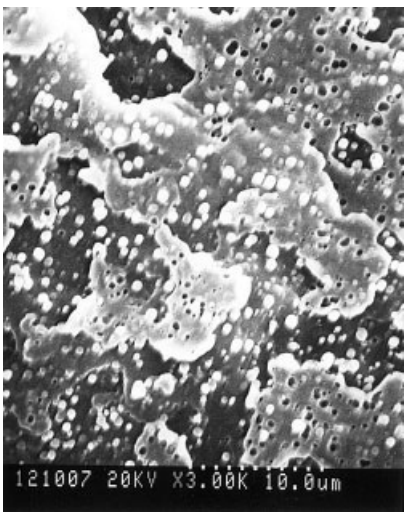

Figure 6 Scanning electron micrograph of a cross section of a PP/EVA blend. The measurement sample was the matrix blend (90/10 EVA/PP).

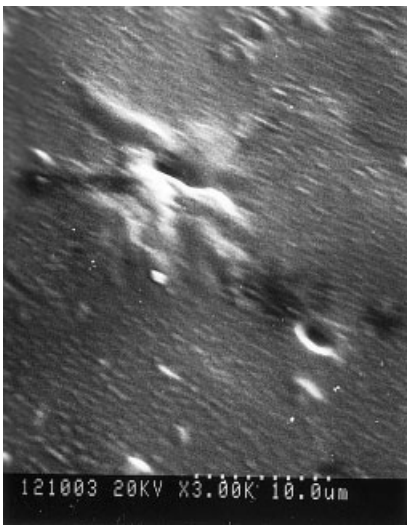

Figure 7 Scanning electron micrograph of the surface of a PP/EVA blend. The measurement sample was the matrix blend (90/10 EVA/PP).

and the extension stress direction decreased, and the plastic deformation stress of the macromolecules increased; the macromolecular segments, which oriented in the fiber, were further stretched, and so the yield strength was higher. At a low rate of deformation, the matrix fiber reached the same microfiber structure when it broke. It could be concluded that the extension at break depended on the initial degree of orientation, and the extension rate at break reached its maximum when the degree of orientation was lower.

Effects of the adsorption time and adsorption temperature on the adsorption amount of the matrix fiber

The matrix fiber adsorbed perfume molecules through the fiber micropores, and the perfume molecules stuck to the active site on the inner surface of the fiber. In this process, the perfume molecules were adsorbed by the matrix fiber with the help of the perfume affinity to the fiber due to the chemical potential difference of the perfume molecules between the solution and the matrix fiber. Figures 6 and 7 show scanning electron micrographs of the cross section and surface, respectively, of a PP/EVA blend (90/10 PP/EVA). The PP/EVA blend was heterogeneous and turned into a sea-island structure. The dispersion-phase EVA was slender and homogeneous in the matrix blends. The matrix fiber was made from PP/EVA blends, and so the matrix fiber was a heterogeneous, melt-spun fiber with a matrix–microfiber structure. The boundary surface between the EVA phase and PP phase was looser because of the poor compatibility between EVA and PP. Some slack appeared between the two phases. The structure of the matrix fiber made the perfume molecules easily adsorbed, diffused, and stored. The ester groups on the side chains of the EVA macromolecules formed an affinity for the active sites of the perfume molecules. With the help of the dipole force and van der Waals force, the matrix fiber adsorbed the perfume molecules. The changes in the amount of the adsorption of benzyl acetate (a kind of perfume molecule) into the matrix fiber (90/10 PP/EVA) with the adsorption time are shown in Figure 8. The concentration of benzyl acetate did not change after 60 min. This showed that the adsorption speed of the matrix fiber was fast for benzyl acetate, and it was related to the morphological structure of the matrix fiber. When the sorption time reached 60 min, the benzyl acetate was completely adsorbed by the matrix fiber, the sorption was saturated, and the amount of sorption did not change anymore with the adsorption time. The changes in the amount of adsorption of benzyl acetate into the matrix fiber (90/10 PP/EVA)

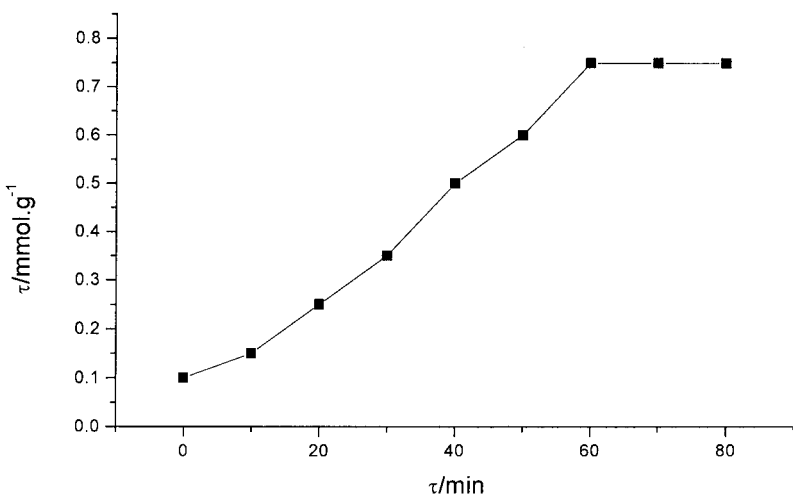

Figure 8 Adsorption of the matrix fiber for benzyl acetate versus time. The measurement sample was the matrix fiber (90/10 EVA/PP).

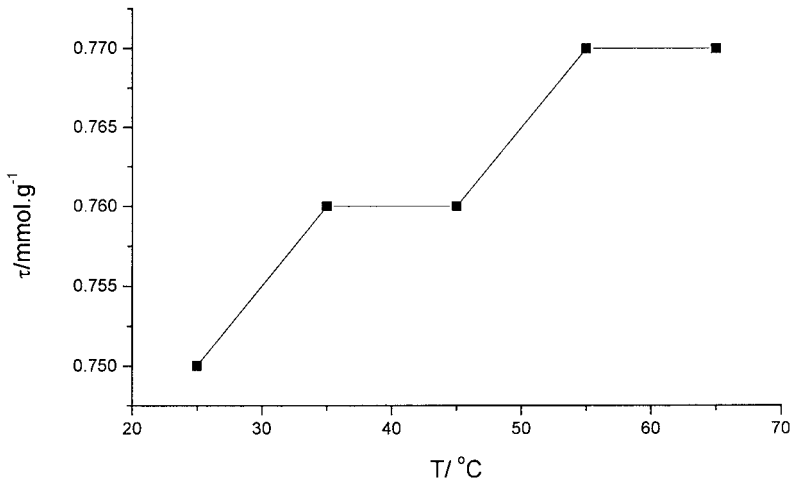

Figure 9 Adsorption of the matrix fiber for benzyl acetate versus temperature. The measurement sample was the matrix fiber (90/10 EVA/PP).

with the adsorption temperature in the same period of time are shown in Figure 9. The amount of adsorption of benzyl acetate into the matrix fiber (90/10 PP/EVA) was fundamentally equal at 25–65°C. The adsorption activation energy of the matrix fiber for benzyl acetate was smaller according to the Arrhenius equation.

Effect of the EVA content on the amount of adsorption of the matrix fiber for perfume molecules

The changes in the amount of adsorption of benzyl acetate into matrix fibers containing different amounts of EVA at 35°C within 60 min are shown in Figure 10. The amount of adsorption of benzyl acetate into the matrix fiber apparently increased with an increase in the EVA content. This illustrated that the amount of adsorption of the matrix fiber mainly depended on the effective EVA content, which contained the active sites for adsorption. The amounts of adsorption of the different perfume molecules into the matrix fiber (90/10 PP/EVA) are shown in Figure 11. The amount of adsorption of benzyl acetate into the matrix fiber (90/10 PP/EVA) was greater than that of dimethyl benzyl methyl acetate into the matrix fiber (90/10 PP/EVA). From the chemical structural formulas of the two kinds of perfume molecules, we find that the benzyl acetate molecule did not have a methyl, but the dimethyl benzyl methyl acetate molecule had two lateral methyls. When the perfume molecules were adsorbed by the active-site ester groups, the dimethyl benzyl methyl acetate was difficult to adsorb because of its steric hindrance, whereas benzyl acetate was easily adsorbed.

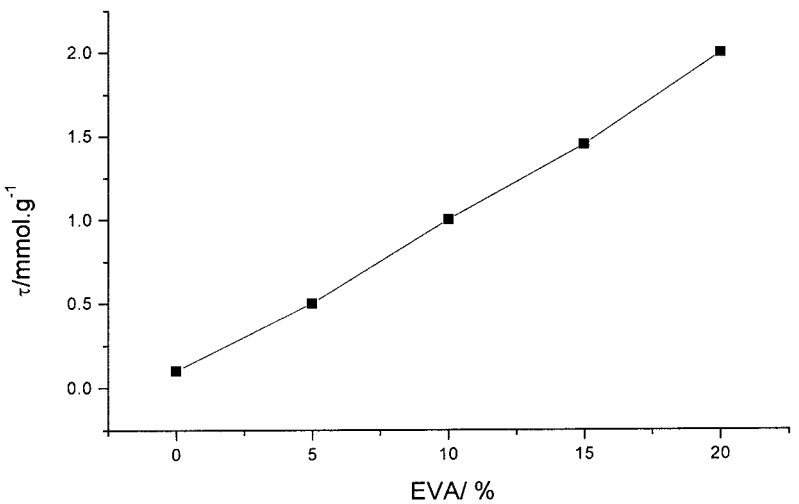

Figure 10 Effect of the EVA content on the adsorption of the matrix fiber for benzyl acetate. The drawing ratio was 2.0, and the heat-treatment temperature was 120–122°C.

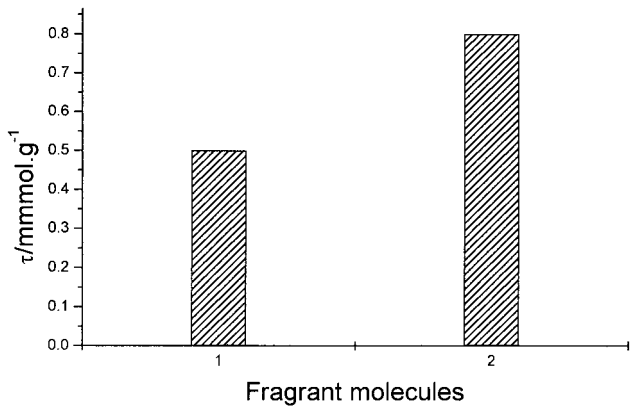

Figure 11 Adsorption of the matrix fiber for different fragrant molecules: (1) dimethyl benzyl methyl acetate and (2) benzyl acetate. The measurement sample was the matrix fiber (90/10 EVA/PP).

Composite adsorption isotherm of the matrix fiber for perfume molecules

Benzyl acetate and absolute alcohol formed a binary liquid-phase mixture. We must consider the effects of the adsorbent (matrix fiber), solute (benzyl acetate), solvent (ethyl alcohol, and boundary surface-oriented molecules when the matrix fiber adsorbed benzyl acetate from the binary liquid-phase mixture. The amount of adsorption of the solution was generally calculated according to the change of one component after adsorption. In fact, the amount of adsorption was a relative amount and also was an apparent amount. Figure 12 describes the composite isotherm of the apparent adsorption of the matrix fiber for a benzyl acetate/alcohol solution. In fact, the apparent isotherm of the adsorption was a composite of the single isothermal curve of benzyl acetate and the single isothermal curve of alcohol; therefore, it was also called a composite isotherm. Generally, there were two kinds of composite isotherms of adsorption, the U type and the S type. In Figure 12, we can see that the composite isotherm of the adsorption of the matrix fiber for benzyl acetate was the U model. The amount of adsorption was an excess in essence. Because there was competitive adsorption between the solute (benzyl acetate) and the solvent (ethyl alcohol), the apparent adsorption amount of the solute (benzyl acetate) that adsorbed into the matrix fiber increased with an increase in the solute (benzyl acetate) molar fraction in the adsorption initial stage. The apparent adsorption amount of the solute (benzyl acetate) that adsorbed into the matrix fiber decreased with a decrease in the solute (benzyl acetate) molar fraction in the later adsorption stage, and the maximum apparent adsorption amount of the solute (benzyl acetate) that adsorbed into the matrix fiber occurred during the adsorption midterm. There have been some reports[17] that the U model composite isotherm can generally be divided into single isothermal curves, and the monolayer adsorption model has generally been used. We could infer the single adsorption isothermal curve of the matrix fiber for a benzyl acetate/alcohol binary liquid-phase mixture with this model. With an increase in the benzyl acetate molar fraction, the single adsorption amount of the matrix fiber for benzyl acetate increased, but the adsorption amount of the matrix fiber for alcohol decreased. If the adsorption were multilayer, there would be still no way of dividing the composite isotherm of the adsorption into a single one.

CONCLUSIONS

EVA and PP crystallized separately according to their own structures in the matrix fiber. Drawing and heat treatment could not make the crystalline structure of

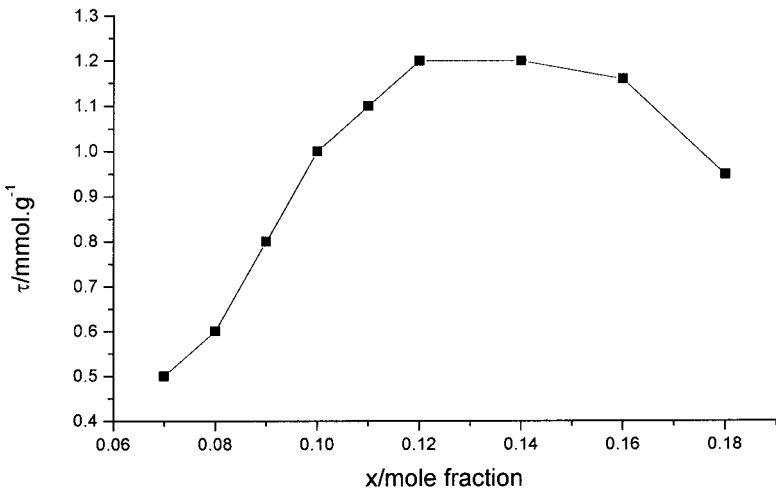

Figure 12 Composite adsorption isotherm of the matrix fiber for benzyl acetate/alcohol. The measurement sample was the matrix fiber (90/10 EVA/PP).

the PP component change and only affected the crystallinity of the PP component. The apparent crystallinity of the matrix fiber was reduced by EVA, and the crystallinity of the component PP increased. The mechanical properties of the matrix fiber were reduced by EVA and increased with an increase in the drawing ratio. The matrix fiber had good adsorption properties for perfume molecules. EVA seriously affected the amount of adsorption of the matrix fiber for perfume molecules. The ester group of the matrix fiber was the active site for adsorption for perfume molecules. The composite isotherm of the matrix fiber for perfume molecules was the U model.

References

1. Xiao, W. Modifications of Synthetic Fibers—Principles and Methods; Chengdu University of Science & Technology: Chengdu, China, 1992.
2. Nakajima, T.; Kajiwara, K.; McIntyre, J. E. Advanced Fiber Spinning Technology; Woodhead: Cambridge, UK, 1994; Chapter 5, appendix.
3. Shen, Y.; Chen, K.; Wang, Q.; Li, H.; Xu, X. J Macromol Sci Chem 1986, 23, 1415.
4. Peterlin, A. J Mater Sci 1971, 6, 490.
5. Zhao, J. S.; Zhou, X. H.; Wang, B.; Tianjin, J. Inst Text Sci Technol 1997, 16(2), 37.
6. Wakahara, H.; Tagawa, K. Jpn. Kokai Tokkyo Koho JP 02 200,876 (90 200,876) (1990).
7. Ichinose, N.; Suzuki, S. Jpn. Kokai Tokkyo Koho JP 02 202,997 (90 202,997) (1990).
8. Wakahara, H.; Tagawa, K.; Nanoo, T. Jpn. Kokai Tokkyo Koho JP 02 185,256 (90 185,256) (1990).
9. Makino, S.; Ito, A. Jpn. Kokai Tokkyo Koho JP 02 221,468 (90 221,468) (1990).
10. Kobayashi, S. Jpn. Kokai Tokkyo Koho JP 2001 62,828 (Cl. B29B7/94) (1994).
11. Koshy, A. T.; Kuriakose, B.; Thomas, S. Polym Degrad Stab 1992, 36, 137.
12. Coran, A. Y.; Patel, R. Rubber Chem Technol 1983, 56, 1045.
13. Jansen, P.; Soares, B. G. Polym Degrad Stab 1996, 52, 95.
14. Kundu, P. P.; Choudhury, R. N. P.; Tripathy, D. K. J Appl Polym Sci 1999, 71, 551.
15. Rohde, E. Kautsch Gummi Kunstst 1992, 12, 1044.
16. Juska, T.; Harrision, I. R. Polym Eng Sci 1982, 22, 766.
17. Kinling, J. J. Adsorption from Solution of Non-Electrolytes; Academic: London, 1965.